The expression used for the temperature distribution was $T = T_e R(\eta)$.

Equation (14a) for F is the well-known Blasius equation, and the differential equation for f_0 is of the third order but linear. In the latter, the coefficient α appears. It depends weakly on time, especially in the hypersonic flow. For example, if $8 \leq M_\infty \leq 10$, then $0.3260 \leq \alpha \leq 0.3711$ for $\theta = 5°$, $0.4295 \leq \alpha \leq 0.4792$ for $\theta = 8°$, and $0.4812 \leq \alpha \leq 0.5315$ for $\theta = 10°$. It is important that these variations of α do not cause large fluctuations in the solution for f_0. The dependence of f_0' on η can be seen in Fig. 2, where the variations in f_0' associated with a change in α also are shown. Continuous and broken lines represent solutions for $\alpha = 0.3260$ and $\alpha = 0.3711$, respectively.

Another coefficient appears in Eqs. (15), namely, κ. The first approximation of the temperature distribution depends on this coefficient. For $8 \leq M_\infty \leq 10$ and for $\theta = 5°$, the value of κ changes from 3.0752 to 3.6389. The corresponding extreme distributions of the R function are shown in Fig. 2. Significant variations in the value of R, of approximately 10%, occur near the wall. Furthermore, the refinement of the solution by the second approximation, which bears the same coefficient, appeared to be relatively insignificant. Consequently, it was decided to terminate calculation of the temperature with the first approximation.

Utilization of Solutions

The shear stress at the wall is given by

$$\tau_w = \frac{c\, p_e U_e}{(c_p - c_v)\rho_\infty} \left(\frac{U_e}{2\bar{\nu}x}\right)^{1/2} \left[F''(0) + \sum_{i=0}^{\infty} f_i''(0)\xi_i\right] \tag{21}$$

where c is the constant relating absolute viscosity with the temperature $\mu = ct$. For the second approximation,

$$\tau_w = \frac{c\, p_e U_e}{(c_p - c_v)\rho_\infty} \left(\frac{U_e}{2\bar{\nu}x}\right)^{1/2} \left[F''(0) + \frac{xU_e'}{U_e^2} f_0''(0)\right] \tag{22}$$

where $F''(0) = 0.4696$ and $1.3376 \leq f_0''(0) \leq 1.3566$.

Numerical Procedure

To solve Eqs. (14) with the associated boundary conditions, the Runge-Kutta method has been used. The step size was assumed to be 0.01, and the limits of integration in η were $\eta = 0$ and $\eta = 20$. Solution of Eq. (15a) could be expressed by quadrature. Numerical evaluation of the integrals expressing function R was done by the use of Simpson's method. Using a procedure based on the method suggested by Moore,[1] the linear equation (14b) was solved relatively quickly. While searching for the function f_0, it was assumed that $f_0 = af_{hom} + f_{inh}$. Here f_{hom} is the solution of Eq. (14b) with the boundary conditions given by $f_{hom}(0) = 0$, $f_{hom}'(0) = 0$, and $f_{hom}''(0) = 1$; and f_{inh} is the solution of Eq. (14b) with the conditions given by $f_{inh}(0) = f_{inh}'(0) = f_{inh}''(0) = 0$. After finding these two solutions, the constant a was obtained according to $a = -\lim_{n\to\infty} f_{inh}/f_{hom}$.

Conclusions

The proposed method enables one to compute relatively quickly the parameters associated with the hypersonic flow around the wedge. The numerical solutions can be used not only for one specific problem but also for a family of problems. This is because the coefficients in the governing equations may be determined a priori from the known or assumed variations in the Mach number and in the angle θ. Velocity of the wedge enters into the solution scheme only in its final phase.

The proposed method can be used only when the parameters $\xi_i (i = 0,1,...)$ are small. In order to meet this condition, the wedge velocity $U(t)$ must be large, but its time derivative should be sufficiently small. In addition, the region of interest should be not too far from the edge of the wedge. For the regions that are further from the edge of the wedge, but in the neighborhood adjacent to the region of our solution, the governing differential equations can be solved numerically also. Here our solution serves as the boundary condition at the initial value of x.

Acknowledgments

This research was supported by the National Research Council of Canada under Grant NRC A4198. Gratitude is expressed to R. Fraser for her congenial help in assembling this paper.

Reference

[1] Moore, F. K., "Unsteady Laminar Boundary-Layer Flow," NACA TN 2471, 1951, pp. 1-33.

Shock Penetration and Lateral Pressure Gradient Effects on Transonic Viscous Interactions

G. R. Inger*
DFVLR – AVA, Göttingen, W. Germany

Introduction

IN existing interaction theories the impinging shock is usually imposed as a boundary-layer edge condition but its subsequent penetration into the layer and the corresponding lateral interaction-pressure gradient is neglected. This is reasonably accurate in laminar flows because of their well-spread-out response to even weak shocks; however, for turbulent flows the interaction is much more violent and short range and hence the shock penetration and lateral pressure gradient effects may be important. For example, Werle and Bertke[1] found that their interacting supersonic boundary-layer model (which otherwise gives consistently good results in laminar flows) severely misrepresents experimental data and exact Navier-Stokes solutions for separating turbulent flow regardless of the viscosity model, ostensibly due to its lack of account for these effects.

The present paper deals with these features for the case of transonic normal shocks interacting with nonseparating turbulent boundary-layers; although in a lower speed range without separation the results provide useful insight as to their nature and parametric dependence.

Theoretical Model

The flow consists of a known turbulent boundary-layer profile $M_0(y)$ disturbed by a weak normal shock. Our original theory[2] was a small disturbance flow treatment, giving a linearized boundary-value problem surrounding the nonlinear shock discontinuity and underlaid by a thin Lighthill viscous sublayer (Fig. 1a). This model represents the essential features of the mixed transonic character of the nonseparating normal shock/boundary-layer interaction problem *including* lateral pressure gradient effects and is amenable to analytical treatment[2] by obtaining solutions for the three regions shown in Fig. 1a.

Received March 9, 1977; revision received April 13, 1977.

Index categories: Jets, Wakes and Viscid-Inviscid Flow Interactions; Transonic Flow.

*Von Humboldt Visiting Senior Research Fellow, Permanent Address: Dept. of Aerospace and Ocean Engineering, Virginia Polytechnic Institute and State University, Blacksburg, Va. Associate Fellow AIAA.

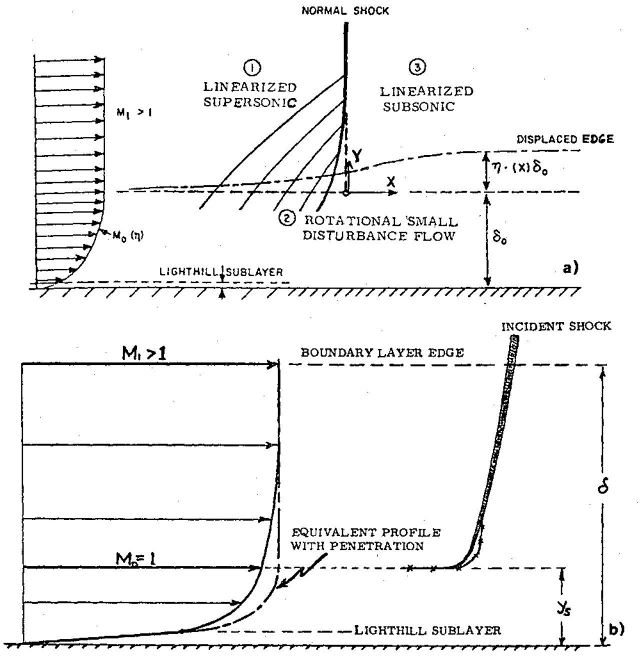

Fig. 1 Interaction flowfield (schematic): a) basic interaction flow model; b) shock penetration region (schematic).

The aforementioned theory assumes the inicident shock is a simple Rankine-Hugoniot discontinuity and also neglects the details of its penetration into the boundary layer; since the correct shock pressure jump at the edge is accounted for while below the sonic level no discontinuity exists, the shock decay across the supersonic nonuniform flow region is in fact roughly simulated by this approximation. However, an improved treatment can be made as follows. Preliminary study shows that except very near the sonic level y_s, the shock angle does not change greatly, primarily decaying in strength as the local Mach number drops. Moreover, since the penetration region $\delta_0 \leq y \leq y_s$ lies in the outer velocity-defect portion of the turbulent profile where the Mach number gradient is weak, this strength decay is also modest except when $y \rightarrow y_s$. Hence a first approximation (and indeed an upper limit) to the penetration effect can be obtained by continuing the incident shock unchanged across the supersonic region. However, to the same order this is simply a "nonpenetrated" interaction solution for an incoming boundary layer having the same skin friction (wall slope) but a smaller thickness $\delta_0' = y_s$ (Fig. 1b), i.e, equivalent to a distortion (primarily in thickness) of the boundary-layer profile. This idea is easily applied by running the existing program twice: the first run establishes $\delta_0, \eta_s = y_s/\delta_0$, C_{f_0}, etc. and the associated "unpenetrated" interaction field solution, while in the second δ_0 is multiplied by η_s wherever it appears in calculating the Mach number profile, Lighthill sublayer properties, etc., taking care *not* to change C_{f_0}.

Discussion of Results

Typical solutions are illustrated in Fig. 2 for both the edge and wall pressure distributions. It is seen that the shock-induced lateral pressure gradients are significant within a region of several boundary-layer thicknesses upstream and downstream of the shock foot. Note that the local shock jump at the edge and its rapid lateral smoothing across the underlying subsonic flow region that yields continuous wall pressure are important physical features that *cannot* be accounted for without the lateral pressure gradient effect. Indeed, the former provides a check against other theories and experiment: Figure 3 shows the good agreement between the predicted local interaction-pressure jump vs shock strength and a variety of data[3] for unseparated flow ($M_1 < 1.3$), correctly approaching the inviscid Rankine-Hugoniot value with increasing M_1 or Reynolds number.

Inclusion of lateral pressure gradients captures another interesting feature verified by experiment: a subsonic post-shock expansion region at the boundary-layer edge due to sign change across the shock of the upstream compression waves from the interaction-induced boundary-layer thickening. This is important in sorting out various theories, since for example transonic flow past a curved wall can also have a post-shock pressure dip due to a purely *inviscid* logarithmic singularity[4]; to properly distinguish these requires consideration of $\partial p/\partial y$.

The penetration effect on the wall pressure field is shown in Fig. 2a (other details are given in Ref. 5). For weak shocks

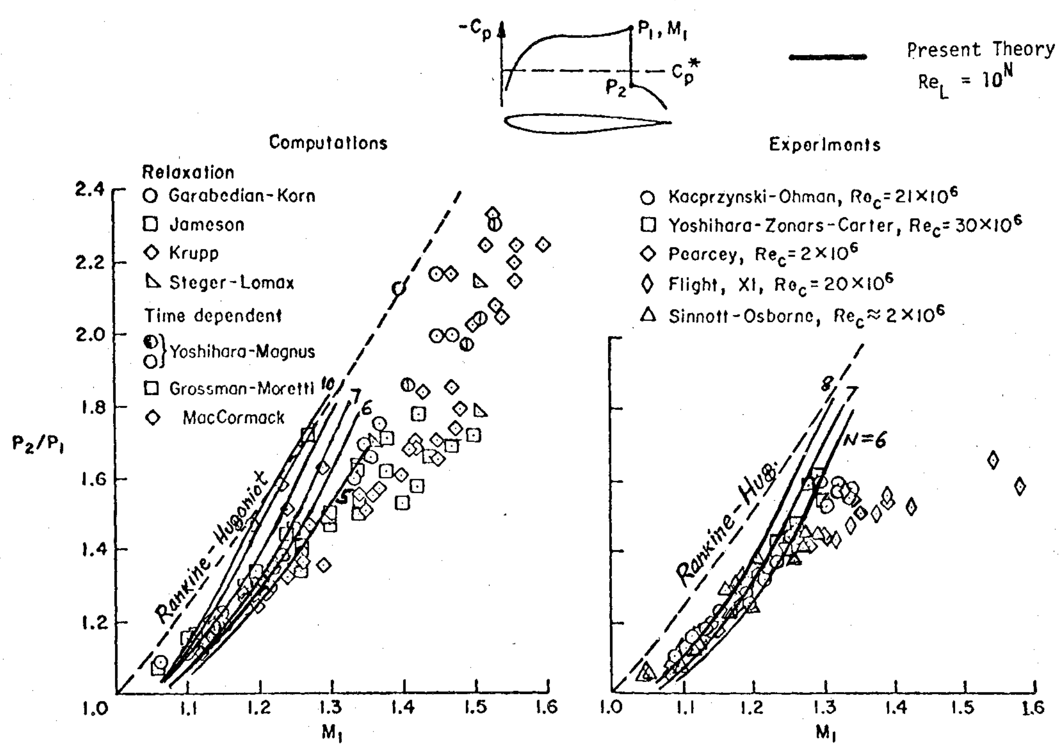

Fig. 2 Shock penetration effect on interaction pressure distributions: a) wall pressure; b) interface pressure.

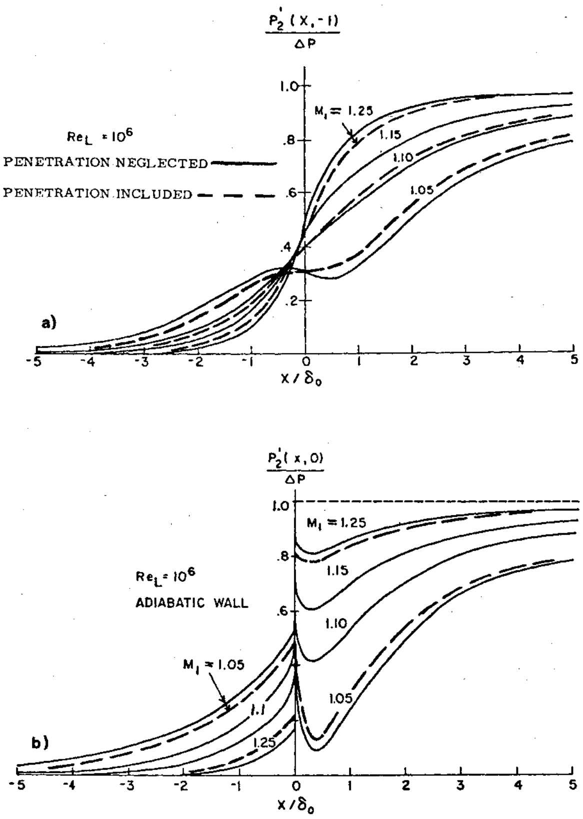

Fig. 3 Local shock jump at boundary-layer edge.

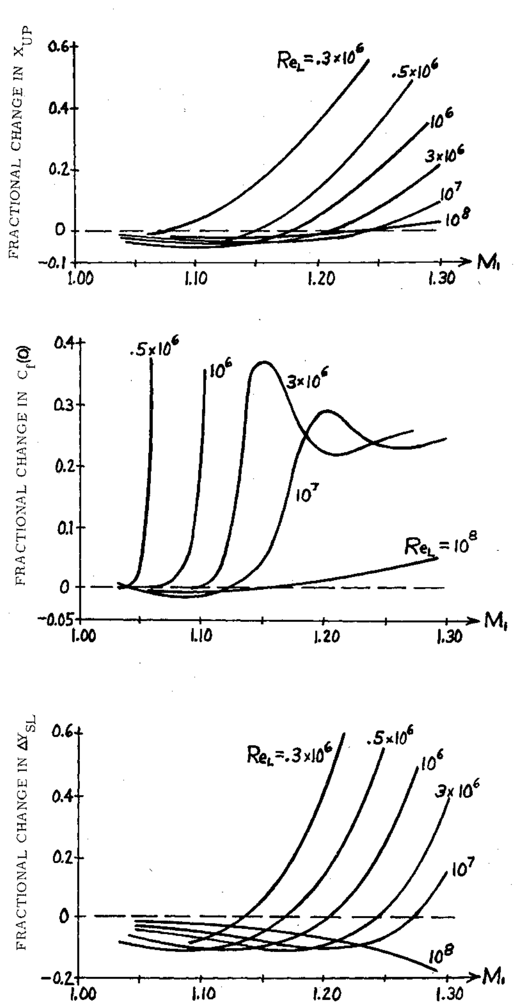

Fig. 4 Shock penetration effects on interaction properties.

($M_1 < 1.15$) the interaction contracts and thins out slightly because the added shock segment acts as an equivalently stronger shock at a slightly higher Mach number, whereas for stronger shocks the reverse occurs and penetration strengthens the interaction by spreading out the streamwise scale, thickening the boundary-layer and reducing the local skin friction. The results of a parametric study of Reynolds number influence are shown in Fig. 4 for the relative changes in upstream influence distance (where $p' = 0.05\Delta P$), skin friction and displacement thickness at the shock foot. These curves further illustrate the intensification of the interaction that occurs with increasing shock strength and also its sensitivity to Reynolds number when $Re_L < 10^8$. For example, while the upstream influence of a $M_1 = 1.20$ shock is increased only 5% by the penetration effect at $Re_L = 10^6$, this becomes 34% at only a slightly lower value $Re_L = 5\times10^5$ (the corresponding thickness effect goes from negligible to 40%).

These trends suggest that the penetration effect increases with shock strength, Mach number, and the onset of separation (equivalent qualitatively to a lower Re_L). This agrees with the finding[1] that omission of this effect in the turbulent case significantly underestimates the strength of the interaction and its streamwise extent, and supports the contention that shock penetration and lateral pressure gradients are important features of interacting high-speed turbulent boundary-layers.

Acknowledgment

This Note is based on research supported by the U.S. Office of Naval Research under contract N 00014-75-C-0456.

References

[1]Werle, M.J. and Bertke, S.D., "Application of an Interacting Boundary Layer Model to the Supersonic Turbulent Separation Problem," University of Cincinnati, Cincinnati, Ohio, Dept. of Aerospace Eng. Report AFL 76-4-21, Aug. 1976.

[2]Inger, G.R. and Mason, W.H., "Analytical Theory of Transonic Normal Shock-Turbulent-Boundary Layer Interaction," *AIAA Journal*, Vol. 14, Sept. 1976, pp. 1266-1272.

[3]Lomax, M., Bailey, F.R., and Ballhaus, W.F., "On the Numerical Simulation Three-Dimensional Transonic Flow with Application to the C-141 Wing," NASA TN D-6933, Aug. 1973.

[4]Oswatitsch, K. and Zierep, J., "Das Problem des senkrechten Stobes an einer gekrümmten Wand," *ZAMM*, Bd. 40, 1960, p. 143.

[5]Inger, G.R., "Shock Wave Penetration and Lateral Pressure Gradient Effects on Transonic Normal Shock-Turbulent Boundary Layer Interactions," VPI & SU, Blacksburg, Va., Report Aero-060, Jan. 1977.

Some Remarks on the Beck Problem

M. S. El Naschie*
University of Riyadh, Saudi Arabia

Introduction

THE buckling of a column under a tangential load (Beck problem) was treated in Ref. 1 using purely static considerations. The buckling load was found to be

$$P_s^c = 20.19\, EI/l^2$$

This value is evidently very close to that obtained by Beck using the dynamic buckling criterion $P_d^c = 20.05\ EI/l^2$. This Note is intended to draw attention to the fact that the value

Received March 3, 1977.
Index category: Structural Stability.

*Assistant Professor.